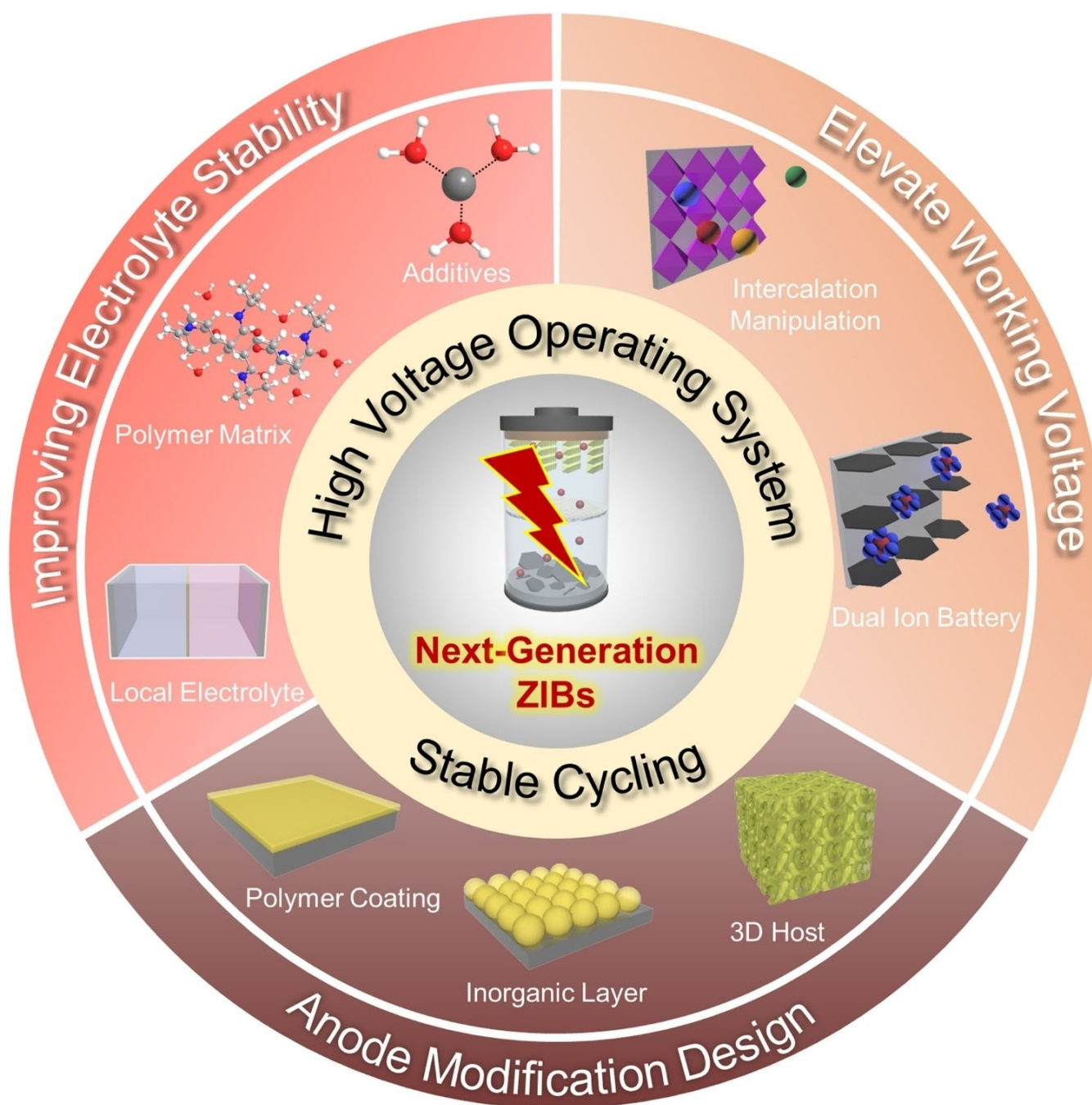


Special Collection

Toward High Energy Density Aqueous Zinc-Ion Batteries: Recent Progress and Future Perspectives

Sangyeop Lee,^[a] Jongha Hwang,^[b] Woo-Jin Song,^{*[b]} and Soojin Park^{*[a]}

Aqueous zinc-ion batteries (ZIBs) are promising next-generation battery system which can mitigate the prevailing issues on the conventional lithium-ion batteries. However, insufficient energy density with low operating voltage prevents the practical utilization of the aqueous system. Notably, aqueous ZIBs suffer from electrolyte decomposition due to its narrow electrochemical stability window (ESW) for 1.23 V. Also, studies on cathode active materials that store charge at an elevated voltage region is still in the initial stage. In this perspective, we

cover the recent strategies for developing high-voltage aqueous ZIBs. First, electrolyte designs for expanding the ESW of an aqueous electrolyte are introduced based on their characterization, materials, and working mechanisms. Next, we propose the cathode active materials with high-working voltage. Furthermore, studies on zinc anodes are also briefly presented. Lastly, we summarize the as-reported strategies and provide insight for developing future ZIBs.

1. Introduction

The depletion of fossil fuels and global efforts toward carbon neutralization have intensified studies on green and renewable energy sources, such as solar, wind, hydro, and tide.^[1–3] In response to the increasing demand for clean energies, the development of large-scale energy storage systems (ESSs) that can effectively store electricity harvested by renewable energy sources is underway to mitigate the uncertainty and intermittency in power generation.^[4,5] Nonaqueous lithium-ion batteries (LIBs), the most widely used energy storage system since its commercialization by SONY in 1991, are a rational approach to ESSs as they provide high energy density, restrained self-discharge, and stable cell cycling.^[6,7] However, potential risk factors including the intrinsic flammability of electrolyte species, unstable supply of electrode material ingredients, and high manufacturing costs remain challenging. Thus, the replacement of conventional nonaqueous LIBs with novel energy conversion and storage systems is urgently required.^[8,9]

Aqueous Zn-ion batteries (ZIBs) based on the Zn metal anode and water-based electrolytes are promising battery systems among post-LIBs, owing to the following beneficial properties: 1) ZIBs possess the fundamental advantages of an aqueous electrolyte including high ionic conductivity, intrinsic nonflammability, and environmental benignity. 2) Zn as an anode material possesses a low electrochemical reduction potential (-0.76 V vs. standard hydrogen electrode) and high theoretical capacity of 820 mAh g^{-1} and 5855 mAh cm^{-3} for gravimetric and volumetric specific capacities, respectively. 3) ZIBs possess economic advantages over other battery systems (Li, Na, Mg, and K) in that they do not require additional inert conditions during manufacturing, owing to the natural water compatibility of the Zn metal anode and low ingredient costs of electrode materials.^[10–12] Nonetheless, the

restrained energy density of ZIBs is a critical challenge that should be overcome to realize the commercialization of ZIBs for ESSs.^[13]

The energy density of batteries can be simply expressed as the product of the specific volumetric capacity and working voltage. Thus, a high working voltage is essential for a high energy density system, but certain obstacles hinder the development of a high working voltage in aqueous ZIBs. According to the water Pourbaix diagram illustrating the relationships among the solution pH, oxygen evolution reaction (OER), and hydrogen evolution reaction (HER) potential, ZIBs unavoidably suffer from a narrow electrochemical stability window (ESW) of 1.23 V for the overall pH region, owing to electrolyte decomposition.^[14] Even considering kinetic hindrance that expands the ESW through the reaction overpotential, aqueous ZIBs still exhibit a cell potential less than 1.7 V, which is considerably lower than that of LIBs based on organic electrolytes (>4.0 V).^[7] Solid electrolyte interphase (SEI) are electronic insulating layer derived from the electrolyte decomposition that suppresses further electrochemical side reactions.^[15] Unfortunately, contrary to the organic electrolytes, aqueous electrolytes are unable to form an *in-situ* SEI layer without adding particular materials and continuous gas evolution can be induced when operated beyond ESW. Furthermore, studies on cathode active materials are another important issue to achieve batteries with high energy density. Notably, the cell voltage can be calculated using the average reaction potential difference between the cathode and the anode. Thus, it is necessary to develop cathode materials that can store charges in a high-voltage region (because Zn metal is mostly utilized as an anode material). Currently, several studies have been recently dedicated to developing aqueous ZIBs with a high working voltage using various strategies.^[16–19] Meanwhile, Zn anode modification is another critical strategy that affects the practical application of high energy density ZIBs. Apparently, anode candidates excepting Zn exhibit inferior properties, which encourages the zinc metal as an indisputable anode material. Hence, it is an inappropriate approach to enhancing the energy density of the battery system. Instead, since the Zn anode affects the cycling behavior of ZIBs, the stabilization of Zn metal should be ensured to fully utilize the operating characteristics of the proposed high-voltage system.^[20,21]

To date, many remarkable reviews have covered electrolyte modification strategies to realize high-voltage ZIBs.^[22–24] How-

[a] S. Lee, Prof. S. Park

Division of Advanced Materials Science and Department of Chemistry
Pohang University of Science and Technology (POSTECH)
Cheongam-ro, Nam-gu, Pohang 37673, Republic of Korea

E-mail: soojin.park@postech.ac.kr

[b] J. Hwang, Prof. W.-J. Song

Department of Polymer Science and Engineering
Chungnam National University
Daehak-ro, Yuseong-gu, Daejeon 34134, Republic of Korea

E-mail: wjsong@cnu.ac.kr

An invited contribution to a Special Collection dedicated to Aqueous Electrolyte Batteries.

Special Collection

ever, an inclusive article dealing with both electrode materials and an electrolyte is still required since an electrolyte with an expanded ESW and advanced electrode materials are equally required to attain high energy density with long-term cyclability. Figure 1 illustrates the challenges in developing a high-voltage system and diverse approaches to alleviate prevailing limitations. Herein, we discuss recent studies on developing high energy density ZIBs based on the expanded cell working potential in terms of electrolyte, cathode, and anode. First, we discuss the electrolyte design for expanding the ESW of an aqueous-based electrolyte using various approaches. Next, structural modification on cathode materials and their underlying mechanism to increase the charge storage voltage are presented. Thereafter, we propose recent advances in Zn anode stabilization and dendrite suppression to support the durable cycling of high-voltage ZIBs. Finally, we summarize the discussed strategies and suggest the remaining challenges and perspectives on the development of the practical application of aqueous ZIBs.

2. Electrolyte Modification for High Voltage Zinc-Ion Batteries

Intrinsically aqueous electrolytes exhibit low electrochemical stability because of water decomposition, where the ESW of water is calculated to be 1.23 V under standard conditions (25°C, 1 atm).^[25] In general, OER and HER occur at the cathode ($\text{H}_2\text{O} \rightarrow 2\text{H}^+ + 1/2\text{O}_2 + 2e^-$) and anode ($2\text{H}^+ + 2e^- \rightarrow \text{H}_2$), respectively, via water decomposition ($\text{H}_2\text{O} \rightarrow \text{H}_2 + 1/2\text{O}_2$).^[26] These side reactions induce critical problems in achieving high-performance ZIBs with high-voltage and long cycle life because they consume electrolytes and increase internal resistance.^[27–29] Table 1 shows the reported electrolyte designs to improve the narrow ESW of aqueous electrolytes.^[30–41] Herein, we discuss

strategies to suppress water decomposition for the broad ESW of aqueous electrolytes and high operating voltage in ZIBs, including the optimization of pH, utilization of bication electrolytes, introduction of small-dipole additives, and design of polymer-supported gel electrolytes.

2.1. Liquid-type electrolytes

Recently, various techniques for liquid-phase electrolytes have been used to expand the ESW of an aqueous electrolyte for high-voltage ZIBs through the construction of an ion-selective membrane.^[42,43] It is well known that pH modification at the individual electrodes (cathode and anode) can effectively hinder the suppression of the electrochemical side reaction and modification of the solvation structure.^[36] In detail, the electrolyte modification based on pH manipulation is related to the prevention of water decomposition. Thermodynamically, the HER and OER potential can be expressed by the Nernst equation as follows:

$$\text{HER : } E_{\text{HER}} = E_{\text{HER}}^0 - 0.059 \text{ pH},$$

$$\text{OER : } E_{\text{OER}} = E_{\text{OER}}^0 - 0.059 \text{ pH}.$$

This indicates that the HER and OER potential can be modified by controlling the pH of an electrolyte.^[44] To stabilize the cell system using pH manipulation, Hu and co-workers designed a pH-localized battery system where three types of aqueous electrolytes (alkaline, neutral, and acidic solutions) were separated by two ion-selective membranes (Figure 2a).^[45] Based on the Nernst equation, they adopted alkaline and acidic solutions as an anolyte and catholyte, respectively, to suppress the detrimental gas evolution reactions and expand the narrow ESW. Interestingly, the fabricated cell exhibited a high open-circuit voltage of 2.8 V, which was considerably higher than the



Sangyeop Lee received his B.S. in Energy Engineering from Ulsan National Institute of Science and Technology (UNIST) in 2018. He is currently M.S.-Ph.D. integrated course student in the Division of Advanced Materials Science at POSTECH. His research focuses on the material design for aqueous battery system.



Jongha Hwang is a M.S.-Ph.D. integrated course student in the department of Polymer Engineering at Chonnam National University. He received his B.S. in Polymer Engineering in 2015. His research focuses on design and synthesis of polymer materials for energy-storage devices.



Prof. Woo-Jin Song received his Ph.D. from the School of Energy and Chemical Engineering at UNIST. He spent one year as a postdoctoral researcher at Stanford University. Now he is an assistant professor in the Department of Organic Materials Engineering at Chungnam National University. His research interests include synthesis of polymer materials for energy-storage-devices and design of next-generation batteries such as flexible/stretchable batteries and aqueous zinc-ion batteries.



Prof. Soojin Park received his Ph.D. in Chemistry from POSTECH. After he spent three years as a postdoctoral research associate at University of Massachusetts at Amherst, he joined to UNIST in 2009, and he moved to Chemistry department at POSTECH in 2018. His research interest includes design of next-generation batteries, synthesis of high capacity anode materials, synthesis of polymeric binder and separator for rechargeable batteries.

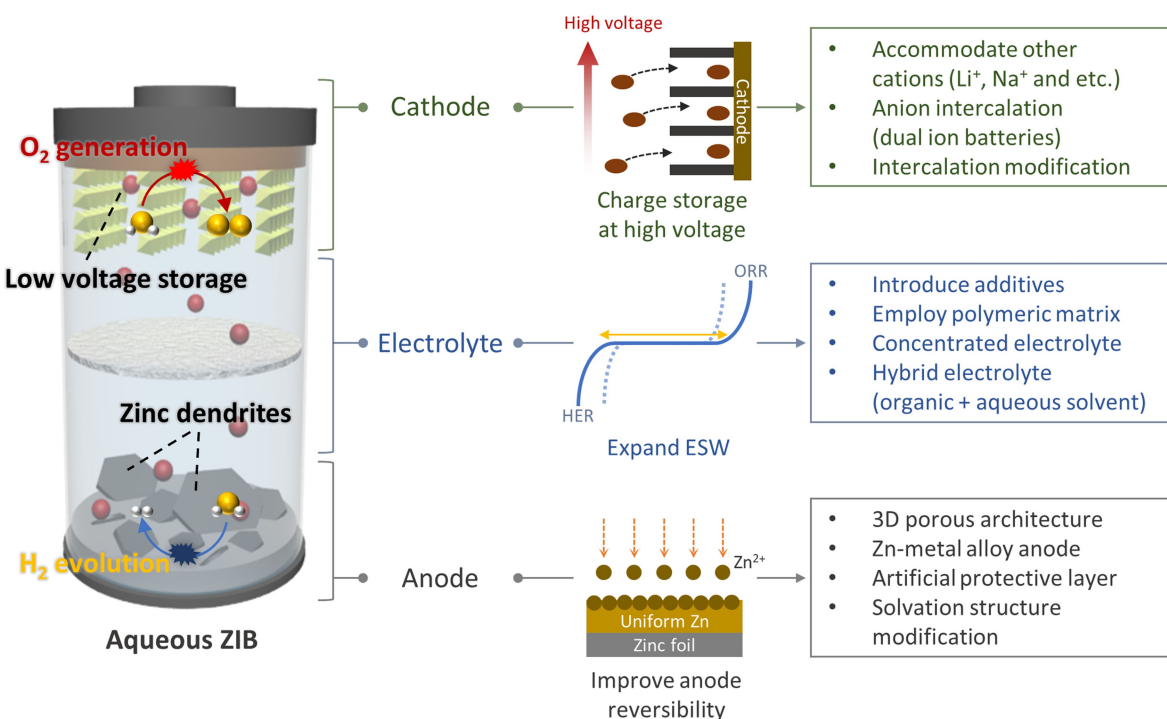


Figure 1. Design strategies to develop durable and high-voltage working aqueous ZIBs.

Table 1. Summary of expanded electrochemical stability window of an aqueous electrolyte for ZIBs.

Type	Electrolyte configuration ^[a,b]	HER potential (vs. Zn/Zn ²⁺) [V]	OER potential (vs. Zn/Zn ²⁺) [V]	ESW [V]	Ref.
pH optimization	1 M Zn(OAc) ₂ + 4 M LiOAc + NH ₃ ·H ₂ O	-1.9	1.0	2.9	[30]
	2 M KOH + 0.02 M Zn(CH ₃ COO) ₂ and 1 M KBr + Br ₂ + 0.5 M H ₂ SO ₄	-1.7	1.4	3.1	[31]
Additive-assisted electrolyte	0.5 M Zn(TFSI) + Acrylamide	-1.2	1.6	2.8	[32]
	1 M Al(CF ₃ SO ₃) ₃ + 1 M Zn(CF ₃ SO ₃) ₂	0.6	2.5	1.9	[33]
Hybrid electrolyte	2 M Zn(BF ₄) ₂ in EMIMBF ₄	-0.1	1.7	1.8	[34]
	1 M Zn(TFSI) ₂ + Acetonitrile	-0.2	2.6	2.8	[35]
Highly concentrated electrolyte	1 M Zn(OAc) ₂ + 31 M KOAC	-1.5	2.0	3.4	[36]
	8 m Zn(ClO ₄) ₂	-1.2	1.6	2.8	[37]
	21 M LiTFSI + 0.5 M ZnSO ₄	-0.3	2.3	2.6	[38]
Hydrogel-based electrolyte	2 M Zn(ClO ₄) ₂ in PEGDM-based hydrogel	-0.1	2.6	2.7	[39]
	1 M NaCl and 1 M ZnCl ₂ in alginate-based hydrogel	-1.4	1.3	2.7	[40]
Molten salts	LiTFSI/acetamide (molar ratio of 1:3.5)/Zn(TfO) ₂ (molar ratio: Li ⁺ /Zn ²⁺ = 20)	-0.5	2.5	3	[41]

[a] The unit M indicates the molarity (mol/L) of the salt concentration. [b] The unit m indicates the molality (mol/kg) of the salt concentration.

theoretical voltage, owing to the liquid junction potential originating from the concentration difference between the electrolytes. Owing to the OER-resistant property, the Zn|MnO₂ battery exhibited a high discharge plateau of 2.71 V at a current density of 100 mA g⁻¹ with a specific capacity of approximately 620 mAh g⁻¹ (Figure 2b). The proposed system was investigated to verify the feasibility of practical large-scale usage, and it successfully achieved an output voltage of 5.44 V and discharge capacity of 6.66 Ah when two cells were connected in series and parallel, respectively (Figure 2c).

In addition, the ESW of an aqueous electrolyte can be expanded using bication electrolytes. For instance, Cheng and colleagues reported bication electrolytes with 1 M Al(CF₃SO₃)₃ + 1 M Zn(CF₃SO₃)₂ to attain a high discharge voltage of 1.7 V in Zn|MnO₂ full cell.^[33] Dissimilar to the electrolyte with single Zn²⁺, the Al³⁺ in the bication electrolytes coordinated with water molecules to form Al(H₂O)_n³⁺ and bound reactive water molecules to suppress gas evolution reactions. During the charge process, the cation of Al³⁺ in the electrolyte responded to the cathode materials upon the removal of H⁺ and Zn²⁺, resulting in the prevention of Mn dissolution for high stability.

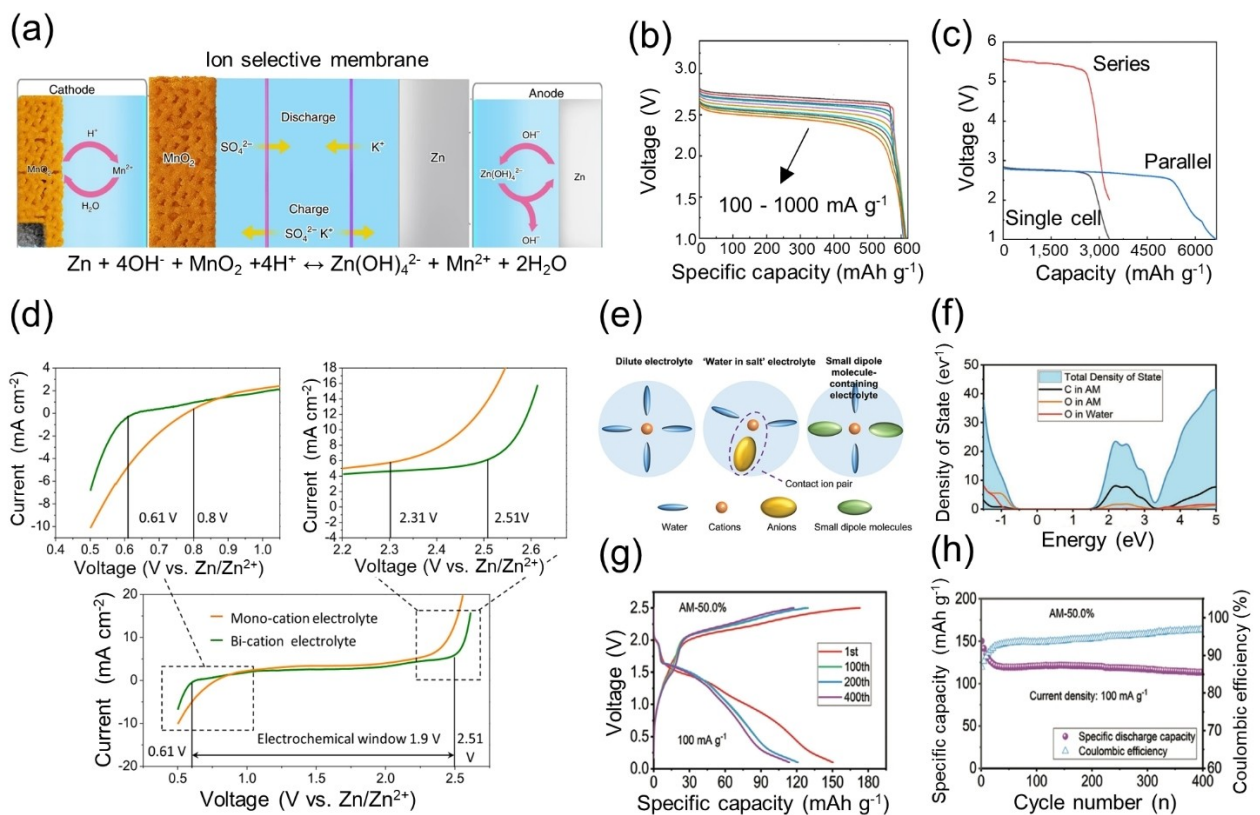


Figure 2. a) The working principle of Zn//MnO₂ battery based on decoupled reactions in acidic and alkaline electrolytes separated by a neutral electrolyte in the central chamber. b) Discharge curves for the decoupled Zn-MnO₂ battery at various discharge current densities. c) Discharge curves of a single and two series-connected decoupled Zn-MnO₂ batteries at a discharge current of 150 mA and 300 mA, respectively. Reproduced with permission from Ref. [45]. Copyright (2020) Springer Nature. d) CV curves and electrochemical window of bi-cation and mono-cation electrolytes at a scan rate of 10 mV/s. Reproduced with permission from Ref. [33]. Copyright (2020) American Chemical Society. e) Schematic image of primary solvation sheath in three kinds of electrolytes. f) The density of state (DOS) of AM-50.0% electrolyte for aqueous ZIBs. g) Galvanostatic charge discharge curves of Zn//LNMO at a current density of 100 mA/g. h) Cycle performance of Zn//LNMO in AM-50.0% electrolyte. Reproduced with permission from Ref. [32]. Copyright (2021) Wiley-VCH.

In addition, trivalent Al³⁺ trapped the Mn ions to form Al_xMnO₂·nH₂O with H₃O⁺ in the Zn|MnO₂ batteries, which could have led to the high discharge plateau. According to the linear sweep voltammetry results in Figure 2(d), the HER potential decreased from 0.8 to 0.61 V (vs. Zn/Zn²⁺), whereas the OER potential shifted from 2.31 to 2.51 V (vs. Zn/Zn²⁺), indicating an expanded ESW in the bication electrolyte. Consequently, compared with the monocation electrolyte (2 M ZnCF₃SO₃)₂), the bication electrolytes exhibited a wider ESW range from 1.5 to 1.9 V. As expected, the Zn|MnO₂ full cell with a bication electrolyte exhibited excellent reversibility with an average Coulombic efficiency of practically 100% and maintained 99.4% of the initial capacity even after 1000 cycles at a charge cut-off of 1.85 V.

Also, small-dipole molecules such as formaldehyde, boron fluoride, thioformaldehyde, and ethylene glycol in the electrolyte can serve a significant role for determining the electrochemical stability of the overall system.^[46–48] For instance, Zhi and coworkers reported the acrylamide (AM)-added electrolytes to develop batteries with remarkable safety and wide ESW (over 2.5 V).^[32] It was reported that small-dipole molecules with high nucleophilicity could effectively enhance the electro-

chemical stability of electrolytes by modifying the solvation sheath of cations, which was further confirmed by the ab initio molecular dynamics (AIMD) simulations (Figure 2e). In an AIMD simulation of the radial distribution function of Zn²⁺ with O in H₂O, the primary solvation sheath of the AM-contained electrolyte was analyzed and revealed that the AM molecules effectively interacted with water molecules to suppress water activity and enhance system stability. Moreover, the redox reaction of the AM molecules preferentially occurred in a small-dipole molecule-induced system because of the electropolymerized olefins of the AM molecules during cycling, confirmed by the states between 1.5 and 3 eV in the density of states (DOS) data (Figure 2f). Consequently, the proposed system exhibited an ESW of 2.81 V, which was fairly improved, compared with the general aqueous electrolyte. Based on the expanded ESW, the proposed full cell achieved a high operating voltage and demonstrated stable cyclability for 400 cycles (Figure 2g and h).

2.2. Gel electrolytes

Firstly suggested by Xu and coworkers in 2015, water-in-salt (WIS) electrolyte systems that utilize extremely concentrated aqueous electrolytes have attracted attention, owing to their improved ESW of 3 V.^[49,50] Understandably, the WIS electrolyte is regarded as a promising system for high-voltage aqueous batteries. However, WIS electrolytes suffer from high viscosity with lower conductivity, expensive ingredients, operating limitations with decreased solubility at a low temperature, and poor electrolyte wettability.^[8,51] Thus, the development of hydrogel electrolytes with the introduction of solvent molecules is a rational approach to overcome as-reported issues for the practical commercialization with a low amount of salt species.^[52,53]

For instance, Ciucci and colleagues reported the cost-efficient hydrated gel electrolyte (HGE) in place of highly concentrated expensive salts (Figure 3a). The poly(ethylene glycol) dimethacrylate (PEGDM)-based structure assisted the formation of gel electrolytes with a strong hydrogen bonding.^[39] The designed HGE exhibited numerous advantages for use in aqueous ZIBs, such as low manufacturing cost, safety, mechanical flexibility, the high solubility of $\text{Zn}(\text{ClO}_4)_2$ salt, the utilization of adiponitrile (AND) as an organic solvent molecule for the large ESW, and electrochemical/thermal stability. In particular, the OER potential shifted from 2.53 to 2.63 V (vs. Zn/Zn^{2+}) in the optimized 2 M $\text{Zn}(\text{ClO}_4)_2$ -based HGE electrolyte (Figure 3b). The Zn^{2+} solvation structures in the HGE electrolyte provided a strong interaction between the water molecules and the polymer matrix to suppress the reactive water, as

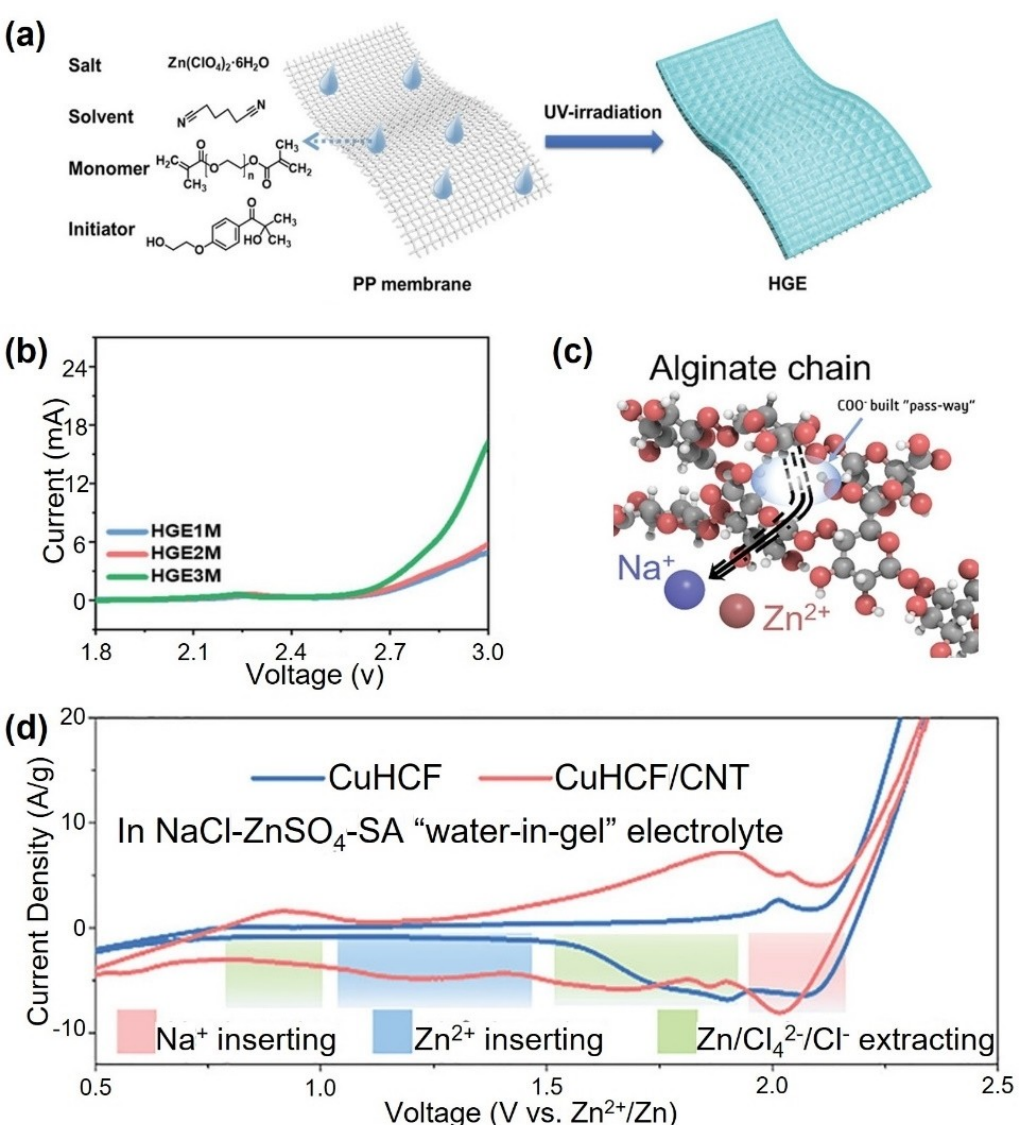


Figure 3. a) Schematic image of hydrogel-based separator fabrication process. b) Linear sweep voltammetry curves of hydrogel-based electrolytes with different salt concentrations. Reproduced with permission from Ref. [39]. Copyright (2021) Wiley-VCH. c) Schematic illustration of ion transportation in the alginate-based hydrogel electrolyte. d) CV curves of CuHCF/CNT cathode with water-in-gel electrolyte. Reproduced with permission from Ref. [40]. Copyright (2021) Wiley-VCH.

confirmed by the density functional theory calculation and AIMD simulation. Thus, the proposed gel electrolyte exhibited a large ESW range of 2.73 V, indicating that the water decomposition was effectively suppressed by introducing hydrated gel polymers.

Furthermore, these gel electrolytes can be adopted for hybrid ion batteries with dual cations. Recently, Leung and coworkers developed a water-in-gel electrolyte using the sodium alginate hydrogel with NaCl/ZnSO₄ dual salt.^[40] The suggested hydrogel structure improved the cation transport behavior by the coordination bonds between the carboxylate groups in the alginate chain and Na⁺/Zn²⁺ ions as described in Figure 3(c). In addition, the strong affinity of sodium alginate reduced the possibility of direct contact between the water molecules and the electrodes via hydrogen bonding. As a result, this gel-derived strategy expanded the ESW to 2.72 V. Furthermore, the alginate-derived hydrogel assisted the high electrochemical stability of Zn²⁺ and Na⁺ intercalation at the copper hexacyanoferrate (CuHCF)/carbon nanotube (CNT) cathode with a high-voltage ion intercalation of 2.3 V (Figure 3d).

In brief, several approaches such as the well-organized dual ions, introduction of multifunctional additives, and polymer architecture can suppress the electrochemical gas evolution reaction originated from water decomposition. Based on the as-reported strategies to expand the ESW of aqueous electrolytes, it is expected that the operating voltage can be increased further and achieve high-energy density aqueous ZIBs in turn.

3. Cathode Designs for High Voltage Zinc-Ion Batteries

Currently, there are various reports on cathode active materials for aqueous ZIBs in terms of an enhanced theoretical specific capacity.^[54–56] Regarding energy density, however, only specific capacity is insufficient, and studies on high-voltage cathodes also should be performed. Meanwhile, classic cathode materials with only Zn²⁺ intercalation reactions exhibit limited working potentials, and cathode materials that can stably accommodate charge transfer carriers in a high-voltage region should be further developed.^[57] Herein, we discuss cathode materials with novel charge carrier intercalation strategies, which realize high-voltage operating batteries with the support of modified electrolyte systems.

3.1. Modification on cation intercalation mechanism

Generally, achieving a high-voltage plateau is important for practical usage and consistent operating performance. Zhi and coworkers recently realized a cathode material for aqueous ZIBs that exhibited a stable voltage plateau at 1.9 V (vs. Zn/Zn²⁺) where 63.5% of the overall capacity originated from the high voltage plateau.^[58] The fabricated LiVPO₄F (LVPF) cathode was decorated with carbon nanotubes (CNTs) and polypyrrole (PPy) to improve the inferior conductivity of LVPF (Figure 4a).

Interestingly, they utilized Li⁺ instead of Zn²⁺ as a cathode-intercalating carrier based on the highly concentrated [21 M LiTFSI + 2 M Zn(OTf)₂] dual-ion aqueous electrolytes. As described in Figure 4(b), the proposed system exhibited the intercalation/deintercalation of Li⁺ during cell cycling, while added Zn salts contributed to the plating/stripping of the Zn anode. In general, Zn²⁺ experiences sluggish intercalation kinetics due to a large solvation sheath and multivalent charge, which restricts the use of widely studied Li-based cathode materials.^[59,60] However, the suggested mixed cation-based Li⁺ intercalation enabled the use of more practical cathode materials via an enhanced charge storage process while maintaining the intrinsic benefits of aqueous ZIBs. The authors conducted *ex-situ* X-ray diffraction (XRD) analysis and revealed that LiVPO₄F underwent phase transformation from Li_xVPO₄F as an intermediate phase to the fully delithiated VPO₄F. In addition, the Li cation accommodating behavior was confirmed by electrochemical measurements which showed that the LVPF cell without Li salts failed to provide charge storage. To verify the practical application of LVPF as a cathode material, electrochemical qualification was estimated using voltage profiles under galvanostatic charge-discharge conditions in Figure 4(c). Clearly, LVPF delivered a specific capacity of 146.9 mAhg⁻¹ at a current density of 0.2 Ag⁻¹ with a practically unchanged voltage plateau of approximately 1.9 V in the overall current density range. Furthermore, it maintained 87% of the initial capacity after 600 cycles and delivered an energy density of 236 Wh kg⁻¹, indicating its feasibility for practical usage.

Meanwhile, a study on developing a high-voltage ZIB by suppressing H⁺ intercalation was recently reported.^[61] Polyanion VPO₄F is a promising cathode, owing to its high operating potential, which accommodates Zn²⁺ cations at 1.9 V (vs. Zn/Zn²⁺), while most of the overall capacity (>70%) is attributed to the proton intercalation below 1.9 V, leading to an unstable high working voltage (Figure 4d). Unfortunately, the intercalation of Zn²⁺ and H⁺ is competitive, and the insertion of H⁺ was detrimental, relating to the formation of a layered double hydroxide precipitate on the positive electrode region, which caused a surface impediment and reduced the electrochemical reversibility. To address the proton insertion, the authors introduced a highly concentrated electrolyte with an organic solvent additive. Quasi-elastic neutron scattering revealed that the proposed system could successfully reduce water mobility. The reduced water mobility increased the ESW of water and suppressed the H⁺ insertion into the VPO₄F matrix. Consequently, VPO₄F exhibited an enlarged Zn²⁺ intercalation voltage plateau over 1.9 V, which delivered considerably more than 50% of the overall capacity. In addition, the fabricated Zn-VPO₄F cell exhibited stable charge-discharge behaviors; similar voltage profiles were observed by comparing the 1st and 10th cycles, which can be ascribed to the increased electrochemical reversibility (Figure 4e). Owing to the improved cation storage mechanism, it exhibited a consistent Coulombic efficiency of approximately 100% and retained 82.5% of the initial discharge capacity after 200 repetitive working cycles with a high energy density of 237 Wh kg⁻¹ (Figure 4f).

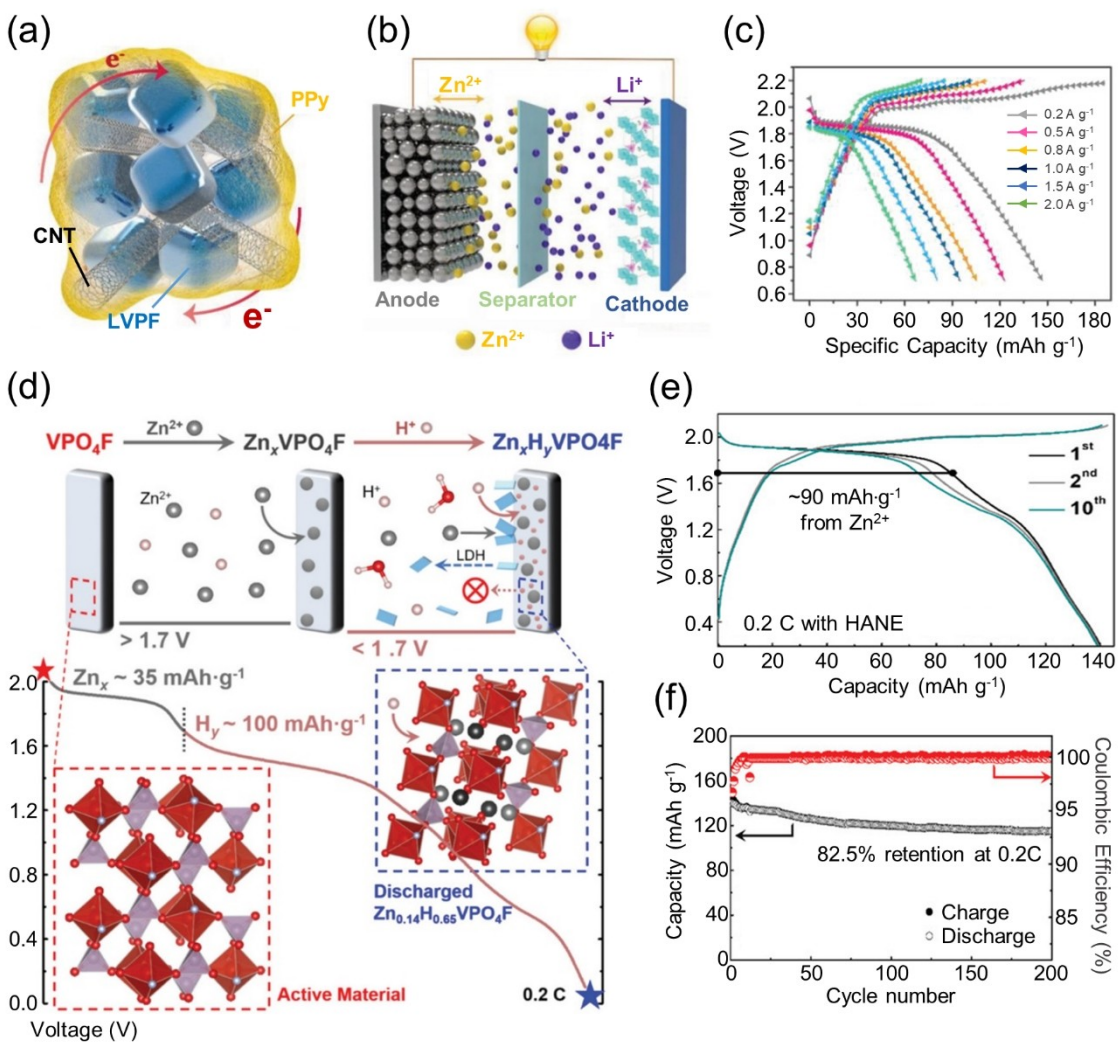
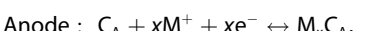


Figure 4. a) Schematic illustration of the CNTs networking and PPy coating for LVPF. b) An illustration of the working mechanism of the Zn²⁺/Li⁺ hybrid battery. c) Galvanostatic charge discharge curves of the battery at various current densities. Reproduced with permission from Ref. [58]. Copyright (2019) Wiley-VCH. d) Schematic of Zn²⁺/H⁺ insertion mechanism during discharge of Zn_xH_yVPO₄F in aqueous electrolyte. At high voltage (> 1.7 V) Zn²⁺ insertion dominates electrochemical activity, but H⁺ intercalation accounts for most of the observed capacity. e) The typical voltage profile of VPO₄F between 0.2 and 2.1 V. f) The typical cycling performance of Zn_xH_yVPO₄ between 0.2 and 2.1 V. Reproduced with permission from Ref. [61]. Copyright (2021) Wiley-VCH.

3.2. Energy storage via anion intercalation

Beyond conventional rechargeable batteries, dual-ion batteries (DIBs) that utilize cations and anions during charge-discharge processes have attracted increasing attention.^[19,62] Interestingly, carbon-based materials (i.e., graphite) serve as a cathode active material in DIBs, and they store energy via anion intercalation in high-potential regions (> 2.1 V vs. Zn/Zn²⁺). As shown in Figure 5(a), cations (Li⁺) and anions (PF₆⁻) intercalate into anode and cathode structures, respectively, during charging, while they are released from the active material structure and migrate back into the electrolyte through a discharge process.^[63] The energy storage and conversion processes of DIBs where graphite serves as both electrodes can be expressed as the following equation:



where C_A and C_C represent the graphite anode and cathode, respectively. M⁺ and Y⁻ indicate the charge carrier metal cationic and anionic species, respectively.^[64]

First reported by Winter et al. in 2012, considerable efforts to adopt dual-ion systems into aqueous ZIBs have been attempted to introduce high-voltage cathodes and enhance energy density.^[65] Notably, in previous studies, the narrow ESW of water impeded anion intercalation reactions, while studies on aqueous-based DIBs have been recently conducted under the guidance of improved electrolyte systems.

For instance, Zafar et al. developed a high-voltage aqueous Zn|graphite DIB based on an 8 m Zn(ClO₄)₂ WIS electrolyte.^[37] They manipulated graphite as a cathode material and con-

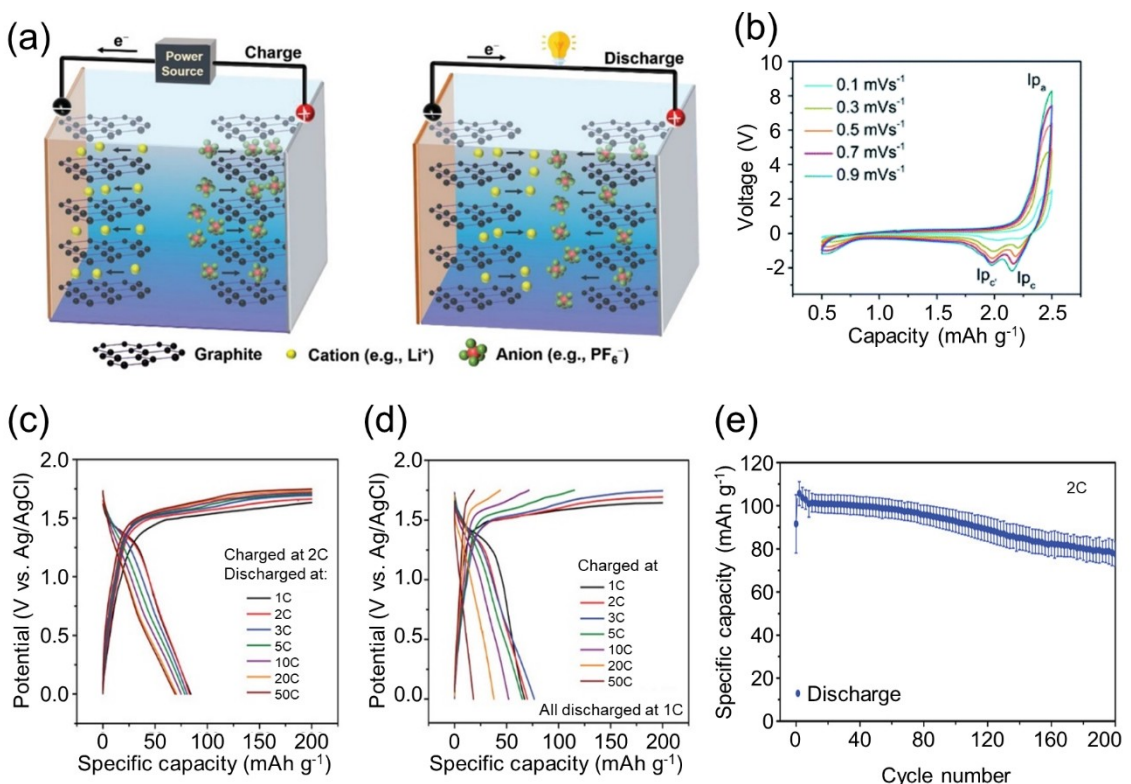


Figure 5. a) Schematic illustration of the charge/discharge mechanism of a typical dual ion battery using graphite as both anode and cathode. Reproduced with permission from Ref. [63]. Copyright (2021) Wiley-VCH. b) CV at different scan rates from 0.1 to 0.9 mV s⁻¹. Reproduced with permission from Ref. [37]. Copyright (2022) Royal Society of Chemistry. c) Galvanostatic charge discharge profiles of graphite charging at a constant current of 200 mA g⁻¹ and discharging at different specific currents of 100–5,000 mA g⁻¹ (1 C:100 mA g⁻¹). d) Charging at different rates of 100–5,000 mA g⁻¹ and discharging at 100 mA g⁻¹. e) Cycling performance at 200 mA g⁻¹ within a cell voltage range of 0.2–2.7 V. Reproduced with permission from Ref. [66]. Copyright (2020) Wiley-VCH.

ducted cyclic voltammetry to determine the working potential (Figure 5b). The fabricated cell exhibited an oxidation peak (I_{pa}) at 2.4 V representing the ClO_4^- intercalation and reduction peaks (I_{pc}) near 2.0 V, attributable to the migration of ClO_4^- anions back into the electrolyte. To demonstrate the intercalation of ClO_4^- into the graphite cathode, *ex-situ* X-ray photoelectron spectroscopy (XPS) was conducted. As expected, XPS confirmed the actual intercalation of charge carrier anions, which was further supported by the *operando* Raman spectroscopy and XRD. Owing to the successful anion intercalation, the Zn|graphite full cell exhibited a high mean discharge voltage of approximately 1.95 V (vs. Zn/Zn²⁺) and stable cycling for 500 cycles at a current density of 100 mA g⁻¹.

Meanwhile, Placke et al. studied the working mechanism of a Zn|graphite DIBs.^[66] In general, it is known that parasitic reactions on the cathode surface and potentially available OERs detrimentally affect the reversibility of the charge-discharge processes and decrease the Coulombic efficiency.^[67] Interestingly, current densities and the Coulombic efficiency strongly correlate in that an enhanced Coulombic efficiency is obtained at high current densities. It is revealed that high charge-discharge rate helps to suppress parasitic side reactions, while kinetically prevalent anion intercalation reactions are preferred leading to deliver higher capacity. As the current continuously

increased, however, a decline in the capacity was observed because of the insufficient charge storage kinetics. Furthermore, they used electrochemical analysis to identify the rate-limiting process during charge-discharge cycles. As illustrated in Figure 5(c and d), cells with different charge currents exhibited diverse capacities even under the same discharge current, while they delivered similar capacities when charged in a fixed current and varying discharge current densities, indicating that the charge process is a rate-limiting step. This was ascribed to the energy storage process of the graphite cathode that graphite layers should be expanded to intercalate anions in the discharged state; therefore, the anion intercalating process became the rate-limiting process. To investigate the feasibility of the Zn-based DIBs, Zn|graphite cells with a “water-in-bisalt” electrolyte were fabricated. As expected, a high average discharge voltage of 2.3 V was observed and demonstrated excellent rate capabilities. Furthermore, the full cell offered a promising cyclability by running for over 200 cycles (Figure 5e).

Table 2 summarizes the as-reported strategies to develop high voltage working cathode materials.^[16,18,31,37,58,61,66,68–76] As illustrated in the table, not only intercalating materials, adopting halogen molecules and p-type organic polymers also can provide high working voltage. It should be further

Table 2. Summary of high voltage working cathode materials for aqueous ZIBs.

Type	Cathode material	Electrolyte configuration ^[a,b]	Working voltage [V]	Specific capacity [mAh g ⁻¹]	Ref.
Zn ²⁺ intercalation/ deintercalation	Zinc hexacyanoferrate	1 M ZnSO ₄ in carboxymethyl cellulose gel	1.85	100	[16]
Zn ²⁺ intercalation/ deintercalation	Cobalt hexacyanoferrate	4 M Zn(OTf) ₂	1.72	173	[68]
Li ⁺ intercalation/ deintercalation	Li ₃ V ₂ (PO ₄) ₃	1 m Zn(OTf) ₂ + 15 m LiTFSI	1.75	126	[69]
Li ⁺ intercalation/ deintercalation	LiVPO ₄ F	2 M Zn(OTf) ₂ + 21 M LiTFSI	1.8	147	[58]
NH ₄ ⁺ intercalation/ deintercalation	Copper hexacyanoferrate	1 M (NH ₄) ₂ SO ₄ · 0.1 M ZnSO ₄	1.8	59	[70]
Zn ²⁺ /H ⁺ co-intercalation/ deintercalation	VPO ₄ F	2 m Zn(OTf) ₂ + propylene carbonate	1.9	140	[61]
TFSI ⁻ intercalation/ deintercalation	Graphite	1.2 M Zn(TFSI) ₂ + acetonitrile	2.2	52	[71]
TFSI ⁻ intercalation/ deintercalation	Graphite	20 m NaFSI + 0.5 m Zn(TFSI) ₂	2.25	110	[66]
ClO ₄ ⁻ intercalation/ deintercalation	Graphite	8 m Zn(ClO ₄) ₂	1.95	45	[37]
OTf ⁻ /TFSI ⁻ co-intercalation/ deintercalation	Graphite	3 m Zn(OTf) ₂ + 21 m LiTFSI	1.7	27	[72]
OTf ⁻ coordination	Thianthrene	1 M Zn(OTf) ₂ + acetonitrile	1.7	110	[18]
Anion coordination	PTVE	1 M ZnSO ₄	1.77	80	[73]
Water coordination	Nickel-ligand coordination grid	1 M KOH + 20 M Zn(CH ₃ COO) ₂	1.8	114	[74]
Conversion	PbO ₂	4 M H ₂ SO ₄ + 0.5 M K ₂ SO ₄ and 6 M KOH + 0.8 M Zn(CH ₃ COO) ₂	2.9	224	[75]
Conversion	I ₂	ZnCl ₂ + LiCl + acetonitrile blend	1.7	300	[76]
Conversion	Br ₂	1 M KBr + Br ₂ + 0.5 M H ₂ SO ₄ and 2 M KOH + 0.02 M Zn(CH ₃ COO) ₂	2.1	395	[31]

[a] The unit M indicates the molarity (mol/L) of the salt concentration. [b] The unit m indicates the molality (mol/kg) of the salt concentration.

mentioned that, although DIB-based aqueous Zn cells delivered high working voltages, they did not demonstrate sufficient capacities, compared with those of cathode materials that use cations as charge transfer carriers. Thus, proper cathode materials are required, which accommodate charge transfer ions in high-potential regions with an enhanced specific capacity to maximize energy densities and realize practical applications.

4. Designs for Anode Stabilization

For the practical realization of high-voltage aqueous ZIBs, the improved reversibility of anode materials is another important factor that affects the stable performance and lifespan of batteries. In particular, the Zn metal anode has attracted the most attention among aqueous ZIBs, owing to its intrinsic benefits. However, the remaining challenges such as HER under aqueous conditions, formation of an insulating layer ($4\text{Zn}^{2+} + 6\text{OH}^- + \text{SO}_4^{2-} + x\text{H}_2\text{O} \leftrightarrow \text{Zn}_4\text{SO}_4(\text{OH})_6 \cdot x\text{H}_2\text{O}$), and dendritic growth restrict the operation of an electrochemically stable Zn metal anode.^[34,77,78] Consequently, many studies have focused on surmounting the as-reported problems. Herein, we present three state-of-the-art strategies to develop a Zn anode with excellent reversibility. First, we suggest the regulation of Zn-ion transfer behaviors. Thereafter, we propose a strategy to control the electric field on the electrolyte/anode interphase. Finally, we introduce the 3D porous structure-based solution to suppress the dendrite growth.

Recently, Guo and coworkers designed a dendrite-free Zn anode by coating a hydrophilic and ionic conductive poly(vinyl butyral) (PVB) artificial interphase layer on Zn foil (Figure 6a).^[79] The coated polymeric layer with favorable hydrophilicity and a high transference number (0.68) effectively suppressed the electrochemical side reactions by preventing the contact of the Zn-solvating water molecules on the anode surface, while Zn²⁺ selectively migrated through the interphase. Furthermore, the stable Zn plating/stripping process by homogeneously distributing Zn ions via a PVB layer was identified by scanning electron microscopy (SEM) (Figure 6b). When assembled in the full cell system, the Zn@PVB anode-based cell exhibited stable charge-discharge voltage profiles and attained excellent capacity retention of 86.6% after 1500 cycles.

In addition to the polymer coating method, adopting metal oxide layers such as TiO₂ and ZrO₂ is regarded as a good strategy to overcome a low cycle performance from the protruding dendrite growth of the Zn metal anode.^[80,81] Unfortunately, this type of protective layer can impede the Zn²⁺ transport with low electrochemical performance because the Zn-ion can only be transferred via cracks and pores.^[82] To address the harmful issues of introducing metal oxides, Li and coworkers used montmorillonite (MMT) as a Zn-ion-conductive SEI layer to suppress dendrite growth and prevent corrosion reactions.^[82] Unexpectedly, the MMT with a high contact angle toward an aqueous electrolyte successively provided the free-way of Zn²⁺ while isolating the bulk electrolyte, owing to the negatively charged MMT lamella structure (Figure 6c), which was electrochemically characterized by the cation transference

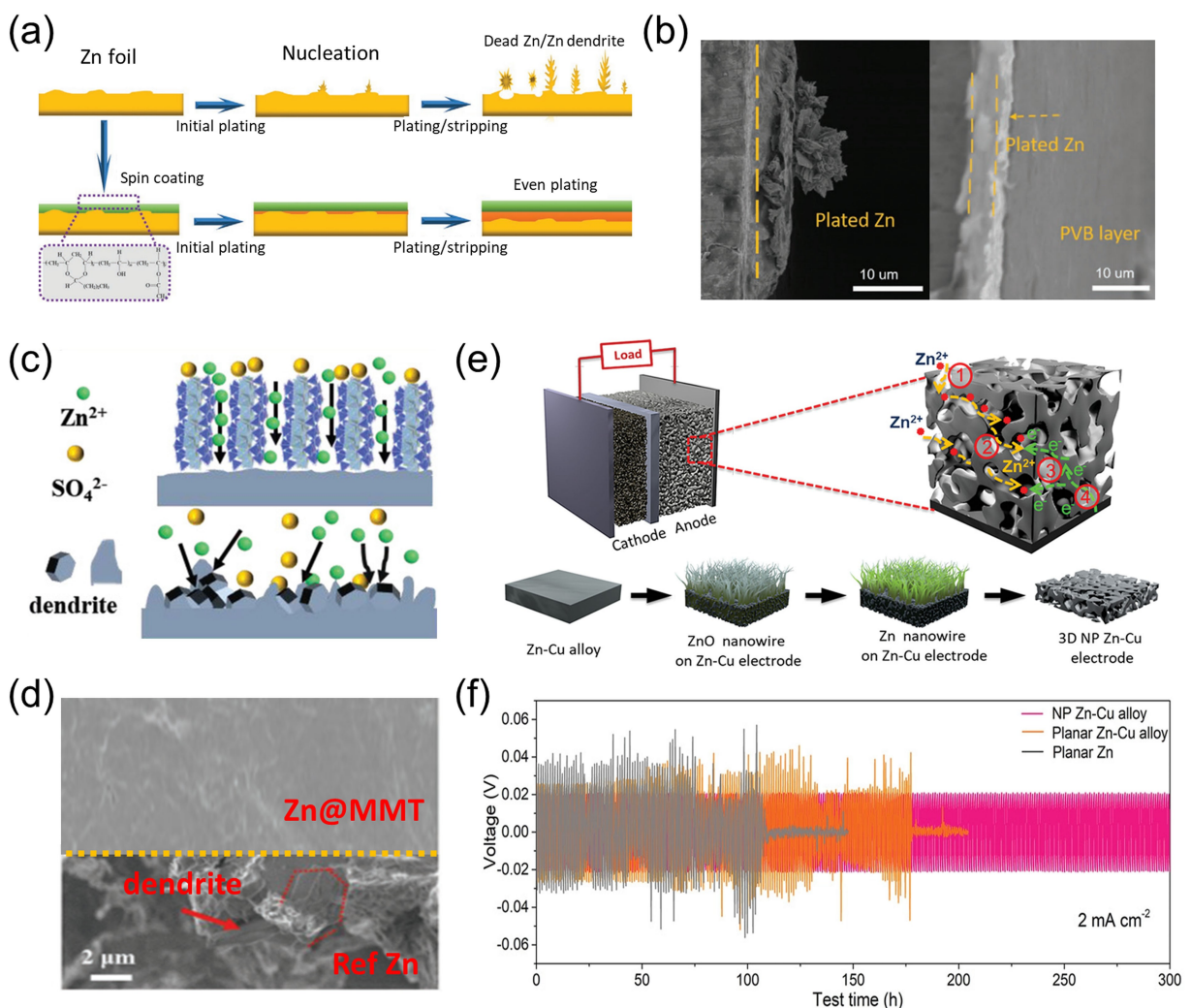


Figure 6. a) Schematic illustration of the formation of Zn dendrite during the Zn plating and stripping process for the bare Zn–Zn cell and the Zn@PVB-Zn@MMT cell. b) SEM images of the surface of plated Zn on the Zn anode (left) and the Zn@PVB (right). Reproduced with permission from Ref. [79]. Copyright (2020) Wiley-VCH. c) The charge-discharge profile of MnO₂/Zn@PVB batteries in 1 M ZnSO₄ and 0.1 M MnSO₄ solution at the rate of 1 C. d) Schematic illustration of the Zn transport mechanism of Zn@MMT. Reproduced with permission from Ref. [82]. Copyright (2021) Wiley-VCH. e) The SEM images of MMT-Zn (up) and Ref Zn (down) anode after 1000 cycles. f) Schematic illustration of the fabrication process of 3D NP Zn–Cu alloy electrode. Reproduced with permission from Ref. [83]. Copyright (2020) Wiley-VCH.

number (the MMT-modified Zn anode showed a value of 0.82, and that of bare Zn ranged between 0.2 and 0.4). As a protective layer, MMT isolated the water molecules from the aqueous electrolyte to adjust the electric field, resulting in a uniform Zn deposition during the charge-discharge process (Figure 6d). Owing to the stabilizing effect, the fabricated full cell exhibited a long cycle life with high capacity. Owing to the stabilizing effect, the fabricated full cell exhibited a long cycle life with high capacity.

Meanwhile, Mai and coworkers proposed a three-dimensional (3D) nanoporous Zn–Cu alloy as an anode for aqueous ZIBs.^[83] Compared with one-dimensional (1D) and two-dimensional (2D) structures, the interconnected 3D architecture with a large surface area possesses the advantages of reducing ion transport resistance, shortening ion diffusion time, and facilitating electron conduction during charge-discharge processes (Figure 6e). As shown in Figure 6(f), the 3D Zn–Cu symmetric

cell achieved a stable plating and stripping process for over 300 h, while the bare Zn and planar Zn–Cu symmetric cell exhibited unstable electrochemical behaviors.

These reliable strategies alleviated the surface side reactions and prevented the dendritic growth of Zn through a homogeneous ion distribution, Zn-selective migration, and the use of multifunctional host materials. We expect that the proposed approaches can provide insight into developing high-performance Zn batteries with stable cycling.

5. Summary and Outlook

ZIBs based on aqueous electrolyte are considered as a promising system to replace the conventional LIBs since they exhibit characteristic advantageous properties such as economic benefits, intrinsic safety, and a convenient manufacturing

process. Currently, research articles about ZIBs mainly focus on improving cell performance and lifetime through electrode material modification, while studies about high voltage aqueous ZIBs beyond 'general aqueous electrolyte' also should be in the spotlight to exceed limited practical application.

In this perspective, we propose the as-reported design strategies to increase working potential of aqueous ZIBs in terms of each component inside the batteries (electrolyte, cathode, and anode). On the one hand, approaches to suppress water decomposition, the most compelling hurdle that restricts widening operating voltage, was introduced. Decreasing the number of reactive water molecules by enhancing interaction between water molecules and electrolyte materials and individualization of pH values in respective electrodes have been reported as effective methods to prevent the gas production. Also, polymer structure contained in gel electrolytes facilely interacts with charge carrier cations and helps to form cation-selective pathway, while blocking direct contact of water molecules on electrode surface. Meanwhile, the potential region storing energy varies according to the type of intercalating species, and thus, it is a promising strategy to increase the working voltage of cathode materials using different charge carriers. In particular, dual ion batteries, which intercalate salt anions like PF_6^- , ClO_4^- , and TFSI^- , have been received attention by many researchers recently owing to its novel operating mechanism and high-voltage reactivity. Lastly, we discussed about zinc anode modification methods for durable and reversible battery systems. Though research on aqueous ZIBs with high operating voltage have been progressed a lot in recent years, it still requires several of improvements for further advancement. Here, we provide some suggestions and perspectives.

1. ESW of an electrolyte is the very factor that determines the working voltage range of the fabricated system and related with the cycling behavior of batteries. As a result, intensive studies on expanding ESW of an aqueous electrolyte is an indispensable work to increase energy density and realize commercialization. Currently, various modification strategies like the use of extremely concentrated salts, the introduction of polymer matrix, the solid-electrolyte system and electrolyte additives are discussed to expand electrolyte ESW. Especially, organic solids such as urea and acetamide can form the eutectic electrolyte with hydrogen bonding network for the broad ESW. Concentrated electrolyte system, known as an efficacious approach to expand ESW by forming unusual solvation chemistry, however, requires metal salts in quantity leading to expensive ingredient costs. Furthermore, they exhibit insufficient ionic conductivity compared with conventional aqueous electrolytes. Consequently, in-depth studies on intermolecular interaction inside the electrolyte and system design that can serve an identical function with much lower concentration is required to fully utilize the advantageous properties of aqueous batteries. Introduction of polymer matrix, additives, and supplemental solvents showed positive potential, however, further research is essential for optimized system between

electrochemical behaviors and economic/industrial viewpoint.

2. Prussian blue analogues, manganese oxides, polyanion species, and organic compounds are all promising cathode active materials for aqueous ZIBs. It is clear that they contributed to the progress on high-performance ZIBs attributed to their cycling stability and feasibility toward high voltage or specific capacity. However, the as-reported cathode materials are insufficient to deliver both high specific capacity and operating voltage simultaneously, and thus, show inferior competitiveness compared with conventional LIBs. Previously, studies on high-voltage working cathode materials attracted less attention due to narrow ESW of aqueous electrolyte. However, many outstanding papers have been reported recently regarding high-performance electrolytes with expanded ESW, and accordingly, research on high-voltage operating cathode materials should be conducted together. For instance, modification on charge transfer carrier can be a rational approach to achieve both high voltage and capacity. Considering that charge storage voltage varies depending on intercalating species, based on the high-capacity cathode material, replacing typical charge carrier (Zn^{2+}) into other cations such as Li^+ , Na^+ , Mg^{2+} , and Al^{3+} is thought to be a feasible research strategy. Also, anion intercalation is a promising approach to enhance working potential, while appropriate type of cathode should be developed to improve deficient specific capacity and maximize the energy density.
3. Alkaline electrolytes with high OH^- concentration can provide a breakthrough to increase energy density of ZIBs because Zn reduction potential decreases below 0 V (vs. Zn/Zn^{2+}) in alkaline condition attributed to the $\text{Zn}-\text{H}_2\text{O}$ Pourbaix diagram. [ref] Furthermore, as introduced in previous section, HER can be suppressed in alkaline solution. Accordingly, alkaline ZIBs such as $\text{Zn}-\text{Ni}$, $\text{Zn}-\text{Ag}$, and $\text{Zn}-\text{Co}$ have been commercialized based on their high energy density and safety.^[84] However, they suffer from severe side reactions between zinc and OH^- anions to form surface insulating species (e.g., ZnO and $\text{Zn}(\text{OH})_2$) during cycling.^[85] Also, high pH values are beneficial in terms of anode stability, while they reduce the onset potential of oxygen evolution restricting the use of high-voltage working cathode materials. As a result, in-depth studies to alleviate cycle deterioration are needed to capitalize on merits of alkaline system. For instance, electrolyte additives can be introduced to prevent electrode dissolution and the formation of surface insulating materials. Furthermore, electrolyte decoupling which adopt acidic catholyte and alkaline anolyte simultaneously is expected to be a rational strategy to develop high-energy density ZIBs.
4. Currently, a good many studies about ZIBs have proved their feasibility in coin-type cells. Coin cells are convenient to manufacture and can provide basic electrochemical properties like specific capacity, working potential and charge/discharge profiles in small size. However, estimating actual behavior in coin cell level is inadequate due to its high internal pressure and low total capacity. Coin cells and

large-scale systems such as cylindrical-, pouch-, and prismatic cells show different electrochemical behaviors and strategies that work in coin cells do not always function equally in 'beyond coin cell' system. Also, even a small amount of gas at the coin cell level is significantly increased in a large area system, and thus, more precise studies on electrolyte decomposition is needed.

Acknowledgements

This work was supported by the National Research Foundation of Korea (NRF-2021M3H4A1A02099354, NRF-2022R1C1C1009974 and NRF-2021M3H4A1A02099354).

Conflict of Interest

The authors declare no conflict of interest.

Keywords: anode stabilization • cathode modification • electrolyte design • high-voltage aqueous batteries • zinc-ion batteries

- [1] A. Hauch, R. Kungas, P. Blennow, A. B. Hansen, J. B. Hanse, B. V. Mathiesen, M. B. Mogensen, *Science* **2020**, *370*, 6513.
- [2] G. Luderer, S. Madeddu, L. Merfort, F. Ueckerdt, M. Pehl, R. Pietzcker, M. Rottoli, F. Schreyer, N. Bauer, L. Baumstark, C. Bertram, A. Dirnachner, F. Humpenoder, A. Levesque, A. Popp, R. Rodrigues, J. Strelfer, E. Kriegler, *Nat. Energy* **2022**, *7*, 32–42.
- [3] B. K. Sovacool, P. Schmid, A. Stirling, G. Walter, G. Mackreron, *Nat. Energy* **2020**, *5*, 928–935.
- [4] X. Guo, Y. Ding, G. Yu, *Adv. Mater.* **2021**, *33*, 2100052.
- [5] H. S. Hirsh, Y. Li, D. H. S. Tan, M. Zhang, E. Zhao, Y. S. Meng, *Adv. Energy Mater.* **2020**, *10*, 2001274.
- [6] F. Wu, J. Maier, Y. Yu, *Chem. Soc. Rev.* **2020**, *49*, 1569–1614.
- [7] A. Manthiram, *Nat. Commun.* **2020**, *11*, 1550.
- [8] Y. Shen, B. Liu, X. Liu, J. Liu, J. Ding, C. Zhong, W. Hu, *Energy Storage Mater.* **2021**, *34*, 461–474.
- [9] L. Yuna, J. Hao, C. C. Kao, C. Wu, H. K. Liu, S. X. Dou, S. Z. Qiao, *Energy Environ. Sci.* **2021**, *14*, 5669–5689.
- [10] T. Zhang, Y. Tang, S. Guo, X. Cao, A. Pan, G. Fang, J. Zhou, S. Liang, *Energy Environ. Sci.* **2020**, *13*, 4625–4665.
- [11] X. Jia, C. Liu, Z. G. Neale, J. Yang, G. Cao, *Chem. Rev.* **2020**, *120*, 7795–7866.
- [12] Q. Zhang, J. Luan, Y. Tang, X. Ji, H. Wang, *Angew. Chem. Int. Ed.* **2020**, *59*, 13180–13191; *Angew. Chem.* **2020**, *132*, 13280–13291.
- [13] B. Tang, L. Shan, S. Liang, J. Zhou, *Energy Environ. Sci.* **2019**, *12*, 3288–3304.
- [14] Y. Yu, J. Xie, H. Zhang, R. Qin, X. Liu, X. Lu, *Small Sci.* **2021**, *1*, 2000066.
- [15] Y. Li, Z. Wang, Y. Cai, M. E. Pam, Y. Yang, D. Zhang, Y. Wang, S. Huang, *Energy Environ. Mater.* **2022**, *0*, 1–29.
- [16] Q. Zhang, C. Li, Q. Li, Z. Pan, J. Sun, Z. Zhou, B. He, P. Man, L. Xie, L. Kang, X. Wang, J. Yang, T. Zhang, P. P. Shum, Q. Li, Y. Yao, L. Wei, *Nano Lett.* **2019**, *19*, 6, 4035–4042.
- [17] V. Soundharajan, B. Sambandam, S. Kim, V. Mathew, J. Jo, S. Kim, J. Lee, S. Islam, K. Kim, Y. K. Sun J Kim, *ACS Energy Lett.* **2018**, *3*, 1998–2004.
- [18] H. Cui, T. Wang, Z. Huang, G. Liang, Z. Chen, A. Chen, D. Wang, Q. Yang, H. Hong, J. Fan, C. Zhi, *Angew. Chem. Int. Ed.* **2022**, *61*, e202203453.
- [19] Q. Guo, K. I. Kim, H. Jiang, L. Zhang, C. Zhang, D. Yu, Q. Ni, X. Chang, T. Chen, H. Xia, X. Ji, *Adv. Funct. Mater.* **2020**, *20*, 2002825.
- [20] Y. Chu, S. Zhang, S. Wu, Z. Hu, G. Cui, J. Luo, *Energy Environ. Sci.* **2021**, *14*, 3609–3620.
- [21] P. Chen, X. Yuan, Y. Xia, Y. Zhang, L. Fu, L. Liu, N. Yu, Q. Huang, B. Wang, X. Hu, Y. Wu, T. V. Ree, *Adv. Sci.* **2021**, *8*, 2100309.
- [22] J. Tan, J. Liu, *Energy Environ. Mater.* **2021**, *4*, 302–306.
- [23] Y. Wang, Z. Wang, F. Yang, S. Liu, S. Zhang, J. Mao, Z. Guo, *Small* **2022**, *2107033*.
- [24] S. Guoa, L. Qin, T. Zhang, M. Zhoua, J. Zhoua, G. Fang S Liang, *Energy Storage Mater.* **2021**, *34*, 545–562.
- [25] H. Zhang, X. Liu, H. Li, I. Hasa, S. Passerini, *Angew. Chem. Int. Ed.* **2021**, *60*, 598–616; *Angew. Chem.* **2021**, *133*, 608–626.
- [26] Y. Li, H. Wang, C. Priest, S. Li, P. Xu, G. Wu, *Adv. Mater.* **2021**, *33*, 2000381.
- [27] Z. Chen, Y. Tang, X. Du, B. Chen, G. Lu, X. Han, Y. Zhang, W. Yang, P. Han, J. Zhao, C. Cui, *Angew. Chem. Int. Ed.* **2020**, *59*, 21769–21777; *Angew. Chem.* **2020**, *132*, 21953–21961.
- [28] L. Ma, N. Li, C. Long, B. Dong, D. Fang, Z. Liu, Y. Zhao, X. Li, J. Fan, S. Chen, S. Zhang, C. Zhi, *Adv. Funct. Mater.* **2019**, *29*, 1906142.
- [29] G. Wang, B. Kohn, U. Scheler, F. Wang, S. Oswald, M. Loffler, D. Tan, P. Zhang, J. Zhang, X. Feng, *Adv. Mater.* **2020**, *32*, 1905681.
- [30] Z. Yu, L. Cao, H. Liu, D. W. Wang, *Energy Storage Mater.* **2021**, *43*, 158–164.
- [31] F. Yu, L. Pang, X. Wang, E. R. Waclawik, F. Wang K Ostrikov, H. Wang, *Energy Storage Mater.* **2019**, *19*, 56–61.
- [32] Z. Huang, T. Wang, X. Li, H. Cui, C. Liang, Q. Yang, Z. Chen, A. Chen, Y. Guo, J. Fan, C. Zhi, *Adv. Mater.* **2022**, *34*, 2106180.
- [33] N. Li, G. Li, C. Li, H. Yang, G. Qin, X. Sun, F. Li, H. M. Cheng, *ACS Appl. Mater. Interfaces* **2020**, *12*, 13790–13796.
- [34] L. Ma, S. Chen, N. Li, Z. Liu, Z. Tang, J. A. Zapien, S. Chen, J. Fan, C. Zhi, *Adv. Mater.* **2020**, *32*, 1908121.
- [35] N. Zhang, Y. Dong, Y. Wang, Y. Wang, J. Li, J. Xu, Y. Liu, L. Jiao, f. Cheng, *ACS Appl. Mater. Interfaces* **2019**, *11*, 36, 32978–32986.
- [36] S. Chen, R. Lan, J. Humphreys, S. Tao, *Energy Storage Mater.* **2020**, *28*, 205–215.
- [37] Z. A. Zafar, G. Abbas, K. Knizek, M. Silhavik, P. Kumar, P. Jiricek, J. Houdkova, O. Frank, J. Cervenka, *J. Mater. Chem. A* **2022**, *10*, 2064.
- [38] J. Zhao, Y. Li, X. Peng, S. Dong, J. Ma, G. Cui, L. Chen, *Electrochim. Commun.* **2016**, *69*, 6–10.
- [39] X. Lin, G. Zhou, J. Liu, M. J. Robson, J. Yu, Y. Wang, Z. Zhang, S. C. T. Kwok, F. Ciucci, *Adv. Funct. Mater.* **2021**, *31*, 2105717.
- [40] W. Pan, Y. Wang, X. Zhao, Y. Zhao, X. Liu, J. Xuan, H. Wang, D. Y. C. Leung, *Adv. Funct. Mater.* **2021**, *31*, 2008783.
- [41] J. Zhang, J. Zhao, H. Du, Z. Zhang, S. Wang, G. Cui, *Electrochim. Acta* **2018**, *280*, 108–113.
- [42] X. Wu, L. Fan, Y. Qiu, M. Wang, J. Cheng, B. Guan, Z. Guo, N. Zhang, K. Sun, *ChemSusChem* **2018**, *11*, 3345–3351.
- [43] X. Luo, X. Lu, G. Zhou, X. Zhao, Y. Ouyang, X. Zhu, Y. E. Miao, T. Liu, *ACS Appl. Mater. Interfaces* **2018**, *10*, 42198–42206.
- [44] F. Wan, J. Zhu, S. Huang, Z. Niu, *Batteries & Supercaps* **2020**, *3*, 323–330.
- [45] C. Zhong, B. Liu, J. Ding, X. Liu, Y. Zhong, Y. Li, C. Sun, X. Han, Y. Deng, N. Zhao, W. Hu, *Nat. Energy* **2020**, *5*, 440–449.
- [46] S. P. Ong, O. Andreussi, Y. Wu, N. Marzari, G. Ceder, *Chem. Mater.* **2022**, *23*, 2979–2986.
- [47] H. Maeshima, H. Moriwake, A. Kuwabara, C. A. J. Fisher, *J. Electrochem. Soc.* **2010**, *157* (6), 696–701.
- [48] Y. H. Tian, G. S. Goff, W. H. Runde, E. R. Batista, *J. Phys. Chem. B* **2012**, *116*, 11943–11952.
- [49] L. Suo, O. Borodin, T. Gao, M. Olguin, J. Ho, X. Fan, C. Luo, C. Wang, K. Xu, *Science* **2015**, *350* (6263), 938–943.
- [50] L. Jiang, L. Liu, J. Yue, Q. Zhang, A. Zhou, O. Borodin, L. Suo, H. Li, L. Chen, K. Xu, Y. S. Hu, *Adv. Mater.* **2020**, *32*, 1904427.
- [51] P. Kulkarni, D. Ghosh, R. G. Balakrishna, *Sustain. Energy Fuels* **2021**, *5*, 1619.
- [52] S. Huang, L. Hou, T. Li, Y. Jiao, P. Wu, *Adv. Mater.* **2022**, *34*, 2110140.
- [53] L. Han, H. Huang, X. Fu, J. Li, Z. Yang, X. Liu, L. Pan, M. Xu, *Chem. Eng. J.* **2020**, *392*, 123733.
- [54] S. Wei, S. Chen, X. Su, Z. Qi, C. Wang, B. Ganguli, P. Zhang, K. Zhu, Y. Cao, Q. He, D. Cao, X. Guo, W. Wen, X. Wu, P. M. Ajayan, L. Song, *Energy Environ. Sci.* **2021**, *14*, 3954–3964.
- [55] Y. Gao, G. Li, F. Wang, J. Chu, P. Yu, B. Wang, H. Zhan, Z. Song, *Energy Storage Mater.* **2021**, *40*, 31–40.
- [56] W. Shi, B. Yin, Y. Yang, M. B. Sullivan, J. Wang, Y. W. Zhang, Z. G. Yu, W. S. V. Lee, J. Xue, *ACS Nano* **2021**, *15*, 1273–1281.
- [57] J. Yan, E. H. Ang, Y. Yang, Y. Zhang, M. Ye, W. Du, C. C. Li, *Adv. Funct. Mater.* **2021**, *31*, 2010213.
- [58] Z. Liu, Q. Yang, D. Wang, G. Liang, Y. Zhu, F. Mo, Z. Huang, X. Li, L. Ma, T. Tang, Z. Lu, C. Zhi, *Adv. Energy Mater.* **2019**, *9*, 1902473.
- [59] Q. Liu, H. Wang, C. Jiang, Y. Tang, *Energy Storage Mater.* **2019**, *23*, 566–586.

- [60] Z. L. Xu, J. Park, J. Wang, H. Moon, G. Yoon, J. Lim, Y. J. Ko, S. P. Cho, S. Y. Lee, K. Kang, *Nat. Commun.* **2021**, *12*, 3369.
- [61] F. Wang, L. E. Blanc, Q. Li, A. Faraone, X. Ji, H. H. C. Mayer, R. L. Paul, J. A. Dura, E. Hu, K. Xu, L. F. Nazar, C. Wang, *Adv. Energy Mater.* **2021**, *11*, 2102016.
- [62] C. Zhang, W. Ma, C. Han, L. W. Luo, A. Daniyar, S. Xiang, X. Wu, X. Ji, J. X. Jiang, *Energy Environ. Sci.* **2021**, *14*, 462–472.
- [63] L. Zhang, H. Wang, X. Zhang, Y. Tang, *Adv. Funct. Mater.* **2021**, *31*, 2010958.
- [64] M. Wang, Y. Tang, *Adv. Energy Mater.* **2018**, *8*, 1703320.
- [65] T. Placke, O. Fromm, S. F. Lux, P. Bieker, S. Rothenmel, H. W. Meyer, S. Passerini, M. Winter, *J. Electrochem. Soc.* **2012**, *159* (11), 1755–1765.
- [66] I. A. R. Perez, L. Zhang, J. M. Wrogemann, D. M. Driscoll, M. L. Sushko, K. S. Han, J. L. Fulton, M. H. Engelhard, M. Balasubramanian, V. V. Viswanathan, V. Murugesan, X. Li, D. Reed, V. Sprenkle, M. Winter, T. Placke, *Adv. Energy Mater.* **2020**, *10*, 2001256.
- [67] L. Jiang, L. Liu, J. Yue, Q. Zhang, A. Zhou, O. Borodin, L. Suo, H. Li, L. Chen, K. Xu, Y. S. Hu, *Adv. Mater.* **2020**, *32*, 1904427.
- [68] L. Ma, S. Chen, C. Long, X. Li, Y. Zhao, Z. Liu, Z. Huang, B. Dong, J. A. Zapien, C. Zhi, *Adv. Energy Mater.* **2019**, *9*, 1902446.
- [69] C. Li, W. Yuan, C. Li, H. Wang, L. Wang, Y. Liu, N. Zhang, *Chem. Commun.* **2021**, *57*, 4319–4322.
- [70] C. Li, J. Wu, F. Ma, Y. Chen, L. Fu, Y. Zhu, Y. Zhang, P. Wang, Y. Wu, W. Huang, *ACS Appl. Energ. Mater.* **2019**, *2*, 10, 6984–6989.
- [71] Z. Chen, T. Liu, Z. Zhao, Z. Zhang, X. Han, P. Han, J. Li, J. Wang, J. Li, S. Huang, X. Zhou, J. Zhao, G. Cui, *J. Power Sources* **2020**, *457*, 227994.
- [72] H. Zhang, X. Liu, B. Qin, S. Passerini, *J. Power Sources* **2020**, *449*, 227594.
- [73] Y. Luo, F. Zheng, L. Liu, K. Lei, X. Hou, G. Xu, H. Meng, J. Shi, F. Li, *ChemSusChem* **2020**, *13*, 2239–2244.
- [74] X. Zhang, J. He, L. Zhou, H. Zhang, Q. Wang, B. Huang, X. Lu, Y. Tong, C. Wang, *Adv. Funct. Mater.* **2021**, *31*, 2100443.
- [75] Y. Xu, P. Cai, K. Chen, Y. Ding, L. Chen, W. Chen, Z. Wen, *Angew. Chem. Int. Ed.* **2020**, *59*, 23593–23597; *Angew. Chem.* **2020**, *132*, 23799–23803.
- [76] Y. Zou, T. Lit, Q. Du, Y. Li, H. Yi, X. Zhou, Z. Li, L. Gao, L. Zhang, X. Liang, *Nat. Commun.* **2021**, *12*, 170.
- [77] J. Hao, X. Li, X. Zeng, D. Li, J. Mao, Z. Guo, *Energy Environ. Sci.* **2020**, *13*, 3917–3949.
- [78] H. Jia, Z. Wang, B. Tawiah, Y. Wang, C. Y. Chan, B. Fei, *Nano Energy* **2020**, *70*, 104523.
- [79] J. Hao, X. Li, S. Zhang, F. Yang, X. Zeng, S. Zhang, G. Bo, C. Wang, Z. Guo, *Adv. Funct. Mater.* **2020**, *30*, 2001263.
- [80] K. Zhao, C. Wang, Y. Yu, M. Yan, Q. Wei, P. He, Y. Dong, Z. Zhang, X. Wang, L. Mai, *Adv. Mater. Interfaces* **2018**, *5*, 1800848.
- [81] P. Liang, J. Yi, X. Liu, K. Wu, Z. Wang, J. Cui, Y. Liu, Y. Wang, Y. Xia, J. Zhang, *Adv. Funct. Mater.* **2020**, *30*, 1908528.
- [82] H. Yan, S. Li, Y. Nan, S. Yang, B. Li, *Adv. Energy Mater.* **2021**, *11*, 2100186.
- [83] B. Liu, S. Wang, Z. Wang, H. Lei, Z. Chen, W. Mai, *Small* **2020**, *16*, 2001323.
- [84] N. Wang, H. Wan, J. Duan, X. Wang, L. Tao, J. Zhang, H. Wang, *Mater. Today* **2021**, *11*, 100149.
- [85] J. Song, K. Xu, N. Liu, D. Reed, X. Li, *Mater. Today* **2021**, *45*, 191–212.

Manuscript received: May 28, 2022

Revised manuscript received: July 15, 2022

Version of record online: July 27, 2022